

Cite this: *Phys. Chem. Chem. Phys.*, 2011, **13**, 12724–12733

www.rsc.org/pccp

PAPER

Raman spectra of long chain hydrocarbons: anharmonic calculations, experiment and implications for imaging of biomembranes

Jiří Šebek,^{†,a} Liat Pele,^{†,a} Eric O. Potma^b and R. Benny Gerber^{*ab}

Received 4th March 2011, Accepted 17th May 2011

DOI: 10.1039/c1cp20618d

First-principles anharmonic vibrational calculations are carried out for the Raman spectrum of the C–H stretching bands in dodecane, and for the C–D bands in the deuterated molecule. The calculations use the Vibrational Self-Consistent Field (VSCF) algorithm. The results are compared with liquid-state experiments, after smoothing the isolated-molecule sharp-line computed spectra. Very good agreement between the computed and experimental results is found for the two systems. The combined theoretical and experimental results provide insights into the spectrum, elucidating the roles of symmetric and asymmetric CH₃ and CH₂ hydrogenic stretches. This is expected to be very useful for the interpretation of spectra of long-chain hydrocarbons. The results show that anharmonic effects on the spectrum are large. On the other hand, vibrational degeneracy effects seem to be rather modest at the resolution of the experiments. The degeneracy effects may have more pronounced manifestations in higher-resolution experiments. The results show that first-principles anharmonic vibrational calculations for hydrocarbons are feasible, in good agreement with experiment, opening the way for applications to many similar systems. The results may be useful for the analysis of CARS imaging of lipids, for which dodecane is a representative molecule. It is suggested that first-principles vibrational calculations may be useful also for CARS imaging of other systems.

1. Introduction

The carbon–hydrogen bond is ubiquitous in biomolecular compounds. In vibrational spectroscopy of bio-organic molecules, the C–H stretching vibrations give rise to band structures that typically constitute the strongest contributions to the vibrational spectrum. These high spectral amplitudes have made the C–H stretching region of the spectrum the premier vibrational range for rapid spectroscopic detection of biologically relevant molecules. In particular, nonlinear Raman microscopy techniques,^{1–3} which enable real-time imaging of cells and tissue materials, make extensive use of the prominent C–H stretching band structures for mapping of lipids, sterols, carbohydrates and proteins. Similarly, the C–H stretching vibrations have been the dominant probes in sum-frequency generation investigations of aliphatic molecules at surfaces.^{4,5}

Despite their central role in vibrational spectroscopy of bio-organic compounds, the link between the vibrational modes and the resulting C–H stretching band profile is not understood in detail. This missing link limits the analytical

capabilities of the vibrational spectroscopic approach. For instance, coherent Raman imaging studies of lipophilic compounds often make use of only one vibrational mode, the symmetric methylene (CH₂) stretching vibration at 2845 cm^{−1},^{6–9} severely compromising the ability to discriminate among different methylene-rich molecular species. Moreover, because the understanding of the subtle balance between symmetric and asymmetric methylene stretches and the corresponding methyl (CH₃) stretches is incomplete, it has been difficult to devise vibrational methods that reliably separate lipids from proteins and/or from carbohydrates. Clearly, a better molecular interpretation of the C–H stretching band would expand the analytical reach of these powerful nonlinear vibrational methods.

The assignment and interpretation of the C–H stretching vibrational range is contingent on the quantitative modeling of the vibrational modes and their mutual couplings in larger molecules. In methylene-rich molecules, the energies of the symmetric and asymmetric modes overlap with overtones and combinational modes, and with Fermi resonances, all of which are sensitive to conformational changes and environmental factors, posing a serious challenge from a modeling point of view. Spectral band assignments have been made based on normal mode analysis methods and a valence force field derived from empirical data.^{10–14} Such models provide a great deal of insights into the basic molecular modes that contribute

^aInstitute of Chemistry and The Fritz Haber Research Center, The Hebrew University, Jerusalem 91904, Israel.

E-mail: benny@f.h.huji.ac.il

^bDepartment of Chemistry, University of California, Irvine, CA 92697, USA

† Authors with equal contributions.

to the band structure, their mutual couplings, and the effects of conformational changes on the Raman band profile. To date, the interpretation of vibrational CARS^{4,15,16} and Raman^{17,18} spectra of methylene rich interfacial molecule layers strongly relies on the band assignments predicted by these empirically inspired normal mode analysis approaches, *cf.* studies of lipid structures and of sum-frequency generation (SFG) measurements.^{4,5}

Yet, a major limitation of the existing assignments of the C–H stretching marker band is that they are based on empirical assumptions, which are difficult to verify. It has, therefore, been complicated to apply band assignments of model systems to C–H-rich biomolecular compounds in general, and to define the quantitative limits of the band positions of the relevant molecular modes. Hence, better models are needed to improve the analytical power of nonlinear vibrational spectroscopy in the C–H stretching range. In principle, detailed *ab initio* calculations can provide the desired information. For the CH band, this requires an anharmonic level of first-principles vibrational calculations. Simple *ab initio* calculations obtained within the harmonic approximation^{19–21} can provide us with valuable information.^{22–24} Their accuracy, however, is not sufficient for detailed analysis of experimental spectra and for utilizing all structural information provided by the experimental spectra.^{25–29} The anharmonic Vibrational Self-Consistent Field (VSCF) method seems to be a very suitable tool for the purpose.

For the analysis of Raman spectra of lipid molecules, the dodecane molecule appears to be a good model system because it is quite a simple molecule containing CH₂ and CH₃ groups, abundant in fatty acids (a very important part of lipid molecules), while the ratio of CH₂ to CH₃ for dodecane and for lipids is similar enough. The *ab initio* calculations involving anharmonic effects enable us to describe the role of symmetric and asymmetric C–H stretches in both CH₂ and CH₃ groups. The VSCF calculations are feasible for dodecane, which enables theoretical analysis of C–H stretches in the frequency region used in the nonlinear Raman spectroscopy. For these calculations we have used the VSCF method and its variants, *e.g.* the vibrational self-consistent field with second order perturbation theory (VSCF-PT2)³⁰ employed for scaled PM3 potential.^{31,32} These methods will be described in the following paragraphs. The calculations and experiments were carried out for both the standard non-deuterated isotopomer of dodecane (C₁₂H₂₆), which is also referred to as H-dodecane, and for the fully deuterated molecule (C₁₂D₂₆)—D-dodecane. Based on this approach and on the comparison of calculations with experiment, a first-principles assignment of the Raman spectra of dodecane will be reached.

The paper is structured as follows: the theoretical and computational methods are described in Section 2. Results and their analysis are the contents of Section 3. Conclusions and remarks are brought in Section 4.

2. Methodology

Raman measurements

Dodecane and deuterated dodecane (d26) were obtained from Sigma-Aldrich and used without further purification. The materials were sandwiched between two borosilicate coverslips

with a 125 µm adhesive spacer. A frequency-doubled Nd: vanadate laser was used to provide 523 nm radiation for the Raman experiments, which was focused by a 20×, 0.75 objective lens onto the sample. Raman scattered light was detected in the epi-direction, filtered by a holographic notch filter and directed to a spectrometer (Andor Shamrock) equipped with a cooled CCD camera (Andor IDus).

Computational methods

Classical molecular dynamics calculations. The geometrical analysis of the molecule of dodecane started with a conformational search with the MM3 force field.³³ Molecular Dynamics simulations were carried out for an isolated molecule at $p = 1$ atm and $T = 295$ K, under isobaric and isothermic conditions (NPT). The use of a thermal ensemble is significant in this case, so as to correspond to the experimental temperature. The Tinker molecular dynamics package³⁴ was used for the calculations.

Ab initio calculations. For all *ab initio* calculations we used GAMESS suite of programs.³⁵ The electronic energies, serving as potentials in the calculation of vibrational frequencies, were generally calculated with the MP2 method³⁶ or an improved PM3 algorithm described below. We generally used the correlation consistent polarized valence double-zeta basis set (CC-PVDZ) proposed by Dunning.^{37,38} The main computational methods used in our study are described in the following paragraphs.

Vibrational self-consistent field (VSCF) methods. Anharmonic interactions including coupling between different modes were treated in this study within the VSCF approach and its extensions.^{39–55} The basic VSCF approach begins with the determination of the normal modes, describing vibrational displacements from the equilibrium structure, as in standard harmonic calculations. Employing other kinds of coordinates is possible.⁵⁶ The VSCF approximation assumes that the full vibrational wavefunction is factorizable into single-mode wavefunctions corresponding to the different normal modes. Equations for the wavefunctions and energy levels of the system are then derived on this basis, while a mean field potential is employed. It represents interactions of each mode with the other modes in the molecule.^{30,57} The full vibrational wavefunctions of the system at the basic level of VSCF are separable, as in the harmonic approximation, but are not harmonic. Unlike the harmonic approximation, the basic VSCF equations are not analytically solvable, but they can be treated quite efficiently numerically.

In VSCF calculations for molecules of this size, it is necessary to approximate the full potential energy. We employ here an approximate representation of the potential function that includes only coupling between pairs of normal modes, neglecting direct interactions of three or more modes.³⁰

VSCF-PT2. Basic VSCF provides improvement over the harmonic approximation, but higher accuracy is obviously desirable. Using second-order perturbation theory for introducing the contributions of the effects beyond wavefunction separability leads to the VSCF-PT2 (VSCF with the Perturbation Theory correction of the second order) algorithm.³⁰ This method is

also often referred to as CC-VSCF (Correlation-Corrected VSCF),³⁰ and Vibrational Møller–Plesset method,⁵⁸ as it is analogous to MP2 from the electronic structure theory.³⁶

Several algorithms for increasing the efficiency of VSCF-PT2 calculations have been used. For example, Pele, Brauer and Gerber suggested a modification using properties of the single-mode VSCF wavefunctions, which greatly improved the scaling of VSCF-PT2 calculations for large systems.^{59,60} Another algorithm suitable for systems where a single transition only in a large polyatomic system is of interest was introduced by Benoit.⁶¹

VSCF methods for vibrationally degenerate states. Results seem to indicate that the consequences of vibrational degeneracy on the accuracy of VSCF calculations are quite often not very severe. Certainly, the effects are of much weaker consequences than is the case for electronic degeneracy in *ab initio* calculations. Several algorithms for dealing with degeneracies have been suggested. One of them, frequently referred to as Vibrational Configuration Interaction (VCI) or D-VSCF (Degenerate VSCF), involves diagonalizing the vibrational Hamiltonian in a VSCF basis, over the degenerate subspace.⁶² A more accurate algorithm called VSCF-DPT2 involves also interactions with non-degenerate states, treated by second-order perturbation theory. Both of these methods are, however, memory and computational time demanding and therefore the calculations are not feasible for molecules discussed here.

A simple approach for solving the degeneracy problem occurring in VSCF-PT2 was introduced by Daněček and Bouř⁶³ and successfully used *e.g.* for mercaptomethane, pyridine and 4-mercaptopuridine.⁶⁴ It is based on modification of the formula used for the second order perturbation correction, which can be justified in case the perturbation is very small. The modified formula does not contain the energy differences between vibrational mode frequencies in a denominator, which is the source of failing of the perturbation theory correction in the case of degenerate systems. This method is referred to as degeneracy-corrected VMP2 (DCVMP2),⁶⁴ in our study we use acronym VSCF-DCPT2, which means degeneracy-corrected VSCF-PT2. We have integrated this method to our GAMESS source code implemented in the same N³ scaling as the VSCF-PT2.

For the quasi-degenerate C–H band of dodecane, we certainly expect Fermi resonance to be present. However, the broadening effects at the room temperature are such that Fermi resonance splittings or shifts are most likely to be washed out by the averaging (the broadening parameters used are 10 cm⁻¹ for part of the transitions, 25 cm⁻¹ for the rest). In fact, as will be seen later, methods that do not treat degeneracy explicitly yield very good accord with experiment. We emphasize here that experiments at low temperatures, under conditions of high-resolution (isolated molecules), are very likely to result in appearance of Fermi resonance manifestations. This is therefore an interesting challenge for the future.

VSCF calculations for *ab initio* potentials. An algorithm for first-principles calculations of anharmonic spectra of polyatomic molecules by direct application of VSCF to potential

surface points from *ab initio* codes was introduced by Chaban, Jung and Gerber.^{45,51,65} *Ab initio* potentials in such calculations are computed for a number of points. This approach is employed here.

Anharmonic vibrational spectroscopy calculations using *ab initio* potentials are too time demanding and are not feasible for our system. However, there are some semiempirical methods that can be efficiently used, *e.g.* PM3.³¹ The accuracy of the semiempirical methods themselves is not sufficient for spectroscopy calculations. However, the accuracy can be much increased by adjusting the PM3 potentials to fit harmonic frequencies from the higher-level *ab initio* MP2 method. The approach used in our research was introduced by Brauer *et al.*³² and has been used and validated by subsequent studies.^{26,66,67} The adjustment of PM3 is accomplished by introducing a scaling, such that

$$V_{\text{scaled}}(Q_1, \dots, Q_n) = V_{\text{PM3}}(\lambda_1 Q_1, \dots, \lambda_n Q_n) \quad (1)$$

where V_{scaled} is the scaled potential, V_{PM3} is the PM3 potential surface, and Q_j is the j th normal-mode coordinate. The scale factor λ_i is determined by the ratio

$$\lambda_i = \omega_{\text{ab initio},i} / \omega_{\text{PM3},i} \quad (2)$$

where $\omega_{\text{ab initio},i}$ is the i th harmonic frequency obtained by the more accurate *ab initio* method, while $\omega_{\text{PM3},i}$ represents the corresponding harmonic frequency obtained by PM3. The λ_i factors are then used for the potential surface calculations, which are a part of the VSCF procedure. Thus, the standard PM3 potential surface in normal coordinates is modified by the scaling of each normal-mode coordinate Q_j by the scale factor λ_i . The idea behind the adjustment of the low-level potential is that the scaled potential has the same harmonic frequencies as the higher-level *ab initio* method. This eliminates a major source of error of the semiempirical potential.

The preconditions for carrying out this scaling procedure include similarities in geometries obtained with PM3 and the higher-level method used and a close correspondence in the nature of the vibrational modes that are being scaled. The proposed scaling makes intuitive sense only if the PM3 normal mode being scaled is similar to the mode obtained by the higher-level method used for scaling.

Raman spectra modeling. The backscattering nonresonance Raman intensities were calculated by a standard formula implemented in GAMESS, the spectra curves were constructed by our software, the temperature was set to 295 K. The intensity expression used is harmonically-derived, the only anharmonic part of the calculation is thus the frequencies. Both the experimental and calculated spectra were normalized selectively to the highest peak.

The VSCF calculations yield sharp transition frequencies. All effects of homogenous and inhomogenous broadening are treated by assuming each transition to correspond to a Lorentzian band, which produces a smoothed spectrum. The Full Widths at the Half-Height (FWHH) were obtained by considerations discussed in the next section.

3. Results and discussion

Analysis of conformers

Some Raman spectra features, especially the spectral band broadening, are strongly dependent on conformation. At room temperature many conformers of organic molecules and biomolecules are present. Therefore a thorough analysis of dodecane conformers has been done. Other spectral factors, causing especially the broadening of bands, e.g. the “hotband” contributions, have not been modeled. The Lorenzian model for the temperature effect is supposed to include all factors. The effect of multiple conformer contributions to the widths was estimated as described below.

7838 conformers of dodecane altogether were found by the MM3 Force Field. Their percentage was calculated from MM3 energies, using the Boltzmann distribution (at 295 K). The global minimum structure (conformer 1 in Fig. 1) is similar to that of fatty acids in lipids. The percentage distribution of conformers at room temperature shown in Table 1 implies that the lowest-energy conformer's population is about 15%, the percentage of each of the first-energy-level conformers (five altogether) is about 3% and the population of each of the other conformers is less than 1%. The vibrational spectra are significantly influenced by the presence of many conformers, a detailed theoretical assessment of this influence is thus not feasible. However, as the stretching vibrations are not critically dependent on the conformation, no other effect than spectral band broadening is supposed to be significant. The MM3 frequency shifts were maximally about 10 cm^{-1} (see Table 1), which shows that the broadening of spectral bands caused by the

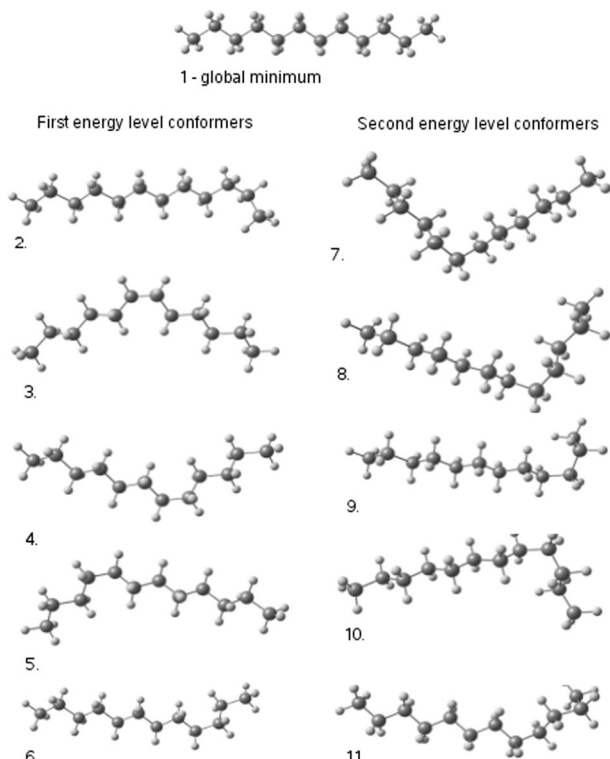


Fig. 1 Conformers of dodecane—the minimum energy structure and the first- and some second energy level conformers.

Table 1 Conformers of Dodecane—the Energy Minimum and the First- and Second Energy Level Conformers—Energies, Percentage and Frequency Shifts in Respect to the Energy Minimum

Conformer	Energy/kcal mol ⁻¹	Percentage	Maximum frequency deviation/cm ⁻¹
1	0.00	14.68	
2	0.84	3.51	6.1
3	0.87	3.35	4.5
4	0.87	3.33	4.5
5	0.87	3.32	4.4
6	0.89	3.24	3.8
7	1.58	0.99	5.6
8	1.59	0.98	5.6
9	1.61	0.94	5.6
10	1.62	0.93	5.6
11	1.67	0.85	5.8
12	1.68	0.84	6.1
13	1.69	0.82	10.8
14	1.69	0.82	4.1
15	1.69	0.82	8.1
16	1.69	0.82	3.9
17	1.70	0.80	6.1
18	1.71	0.80	6.1
19	1.71	0.80	6.1
20	1.71	0.80	6.1
21	1.71	0.79	6.1
22	1.71	0.79	3.4
23	1.71	0.79	11.9
24	1.72	0.78	8.8
25	1.72	0.78	6.1
26	1.72	0.77	6.1
27	1.73	0.76	11.8
28	1.74	0.76	8.7
29	1.74	0.75	5.4
30	1.75	0.75	5.4
31	1.75	0.74	5.3
32	1.76	0.74	4.6
33	1.76	0.73	4.6
34	1.76	0.73	5.4
35	1.77	0.71	4.4
36	1.77	0.71	4.4
37	1.80	0.68	6.8
38	1.84	0.63	5.3
39	1.84	0.63	5.1
40	1.86	0.62	4.5

presence of more conformers is maximally about 10 cm^{-1} . We have thus set the value of the full width at a half-height (FWHH) of most Raman bands in the calculated spectra to 10 cm^{-1} .

For the global minimum energy structure the harmonic vibrational frequencies and Raman intensities in the C–H stretch region were calculated at the MP2/CC-PVDZ level, and the VSCF anharmonic frequencies by the improved PM3 method, while the scaling factors were obtained from MP2/CC-PVDZ and standard PM3 frequencies, according to Formula (2).

The dodecane Raman spectra

The harmonic spectra and assignment of the modes. The harmonic spectra of dodecane are depicted in Fig. 2 (non-deuterated) and Fig. 3 (deuterated). The main spectral experimental patterns are quite well reproduced by the calculations for both isotopomers, despite a significant blue shift (around 200 cm^{-1}), which is a result of neglecting anharmonic effects. This phenomenon is very well-known in the vibrational spectroscopy. However, these results are sufficient for identification of the modes responsible for most of the peaks in the

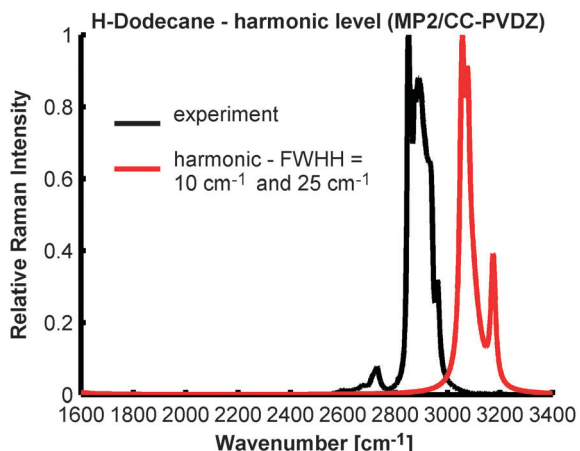


Fig. 2 The harmonic MP2/CC-PVDZ spectra of a non-deuterated dodecane isotopomer (red curve) compared to experiment (black curve).

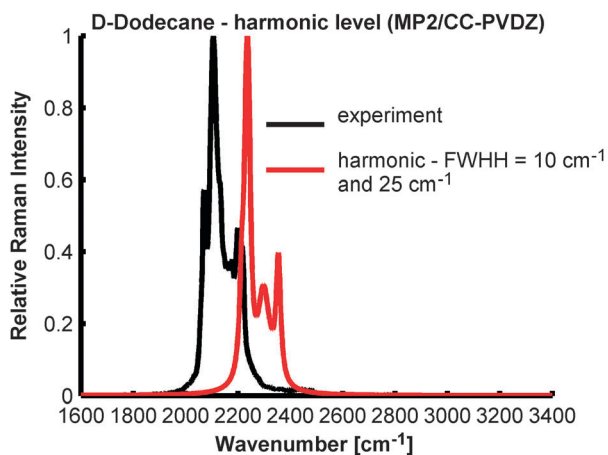


Fig. 3 The harmonic MP2/CC-PVDZ spectra of a deuterated dodecane isotopomer (red curve) compared to experiment (black curve).

experimental Raman spectra. The numbers in Table 2 show a clear separation of all different types of H-dodecane normal modes at the harmonic level (CH_2 symmetric, CH_3 symmetric, CH_2 asymmetric, and CH_3 asymmetric—in the increasing order of their frequencies). As the general experimental experience shows that the CH_2 asymmetric modes are in general very sensitive to their environment and when the local environment becomes more disordered (from solid to liquid), the CH_2 asymmetric modes broaden significantly, while the CH_2 symmetric modes are not so sensitive, the CH_2 asymmetric modes can be expected to be much more broadened (two or three times) than the CH_2 symmetric modes for liquid samples. Hence, we set the value of FWHH for CH_2 asymmetric bands to 25 cm^{-1} , while the FWHH value of the other modes was set to 10 cm^{-1} , due to the conformer equilibria effects, as described above. This smoothing of the lines is a very simple approach to incorporate broadening effects on an otherwise first-principles single molecule calculation at $T = 0 \text{ K}$. Since this leads to good accord with experiment, as we shall see later, it is very encouraging for quantitative calculations of hydrocarbon Raman spectra.

The anharmonic effects. The spectrum obtained by the VSCF method at the improved PM3 level, together with the

Table 2 The vibrational frequencies of the CH_2 and CH_3 stretching modes in the non-deuterated dodecane molecules at both the harmonic and the anharmonic levels

Mode	Type	MP2 harmonic	Imp. PM3-VSCF	Imp. PM3- VSCF_DCPT2	Raman intensities
89	CH_2 sym	3053	2864	2858	1
90	CH_2 sym	3053	2867	2824	20
91	CH_2 sym	3054	2866	2860	0
92	CH_2 sym	3054	2862	2833	1
93	CH_2 sym	3056	2886	2836	511
94	CH_2 sym	3057	2866	2858	0
95	CH_2 sym	3061	2874	2850	19
96	CH_2 sym	3064	2878	2871	0
97	CH_2 sym	3071	2886	2864	92
98	CH_2 sym	3071	2867	2855	1
99	CH_3 sym	3077	2850	2772	8
100	CH_3 sym	3077	2861	2802	332
101	CH_2 asym	3094	2941	2935	372
102	CH_2 asym	3095	2940	2935	1
103	CH_2 asym	3097	2942	2936	47
104	CH_2 asym	3102	2949	2945	0
105	CH_2 asym	3107	2958	2955	33
106	CH_2 asym	3115	2961	2960	0
107	CH_2 asym	3122	2970	2966	39
108	CH_2 asym	3127	2973	2968	0
109	CH_2 asym	3132	2977	2973	28
110	CH_2 asym	3135	2984	2980	0
111	CH_3 asym	3172	2905	2872	70
112	CH_3 asym	3172	2912	2881	1
113	CH_3 asym	3175	2935	2897	52
114	CH_3 asym	3175	2941	2904	144

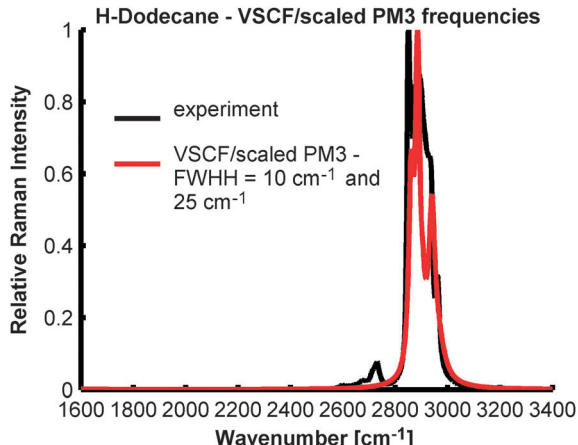


Fig. 4 The VSCF spectra of a non-deuterated dodecane isotopomer calculated with the improved PM3 method (red curve) compared to experiment (black curve).

experiment, is shown in Fig. 4 (H-dodecane) and Fig. 6 (D-dodecane). The agreement of the calculated frequencies with the experimental data is very good. Even the calculated intensities (note that they were obtained harmonically) fit the experiment very well. One of few discrepancies is that one experimental peak at the red edge of the H-dodecane spectrum was not reproduced by the calculations. The possible origins of this peak will be discussed later. To show the contribution of individual transitions and the averaging effects, Fig. 5 and 7 are shown. They depict the calculated H- and D-dodecane VSCF spectrum and the Raman intensities of all C-H and C-D stretches.

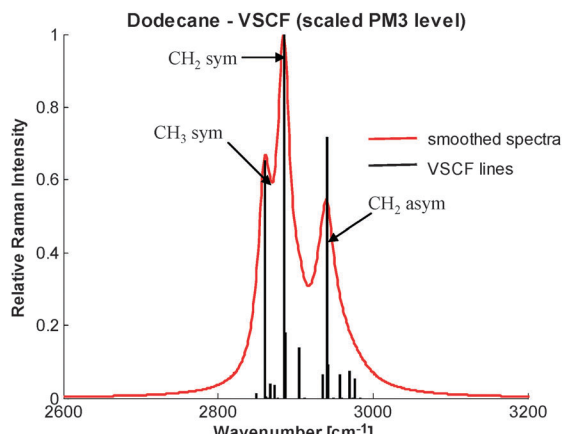


Fig. 5 The smoothed VSCF spectrum of a non-deuterated dodecane isotopomer calculated with the improved PM3 method (red curve) with the VSCF lines corresponding to all fundamental transition in this spectral range (black lines). The position of each black line corresponds to the transition frequency and the height denotes the transition relative Raman intensity (compared to the most intense transition).

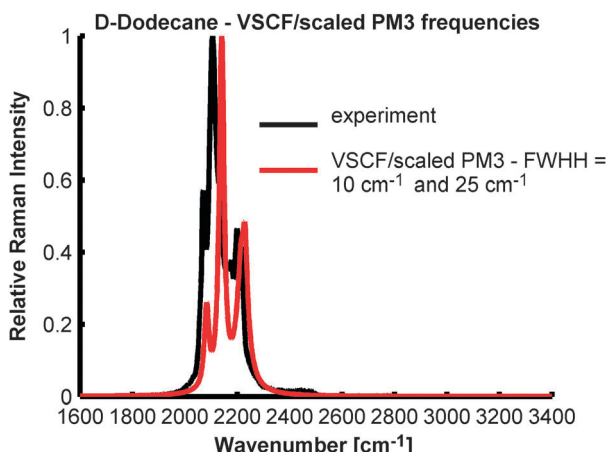


Fig. 6 The VSCF spectra of a deuterated dodecane isotopomer calculated with the improved PM3 method (red curve) compared to experiment (black curve).

The VSCF-DCPT2 method shifts most of the vibrational frequencies to the left and changes the spectral shape quite significantly, see Fig. 8 and 9. The results are similar to those of the VSCF-PT2 version as implemented in GAMESS (not shown), in which terms near to singularity due to degeneracies are dropped. While the DCPT2 correction apparently improves the D-dodecane spectrum, it is questionable if it works so well for H-dodecane. In this case, the position of the transition with the highest calculated intensity seems to correspond to the highest experimental peak much better than for simple VSCF, however, it is also possible that in reality the second largest peak in the calculated spectrum corresponds to the experimental absolute maximum, note that the Raman intensities were calculated harmonically and so a worse accuracy is expected. The other features of the spectral profile seem to be reproduced better by simple VSCF than by VSCF-DCPT2.

Both of the anharmonic methods more or less preserve the separation of the mode types in the spectra, even though they

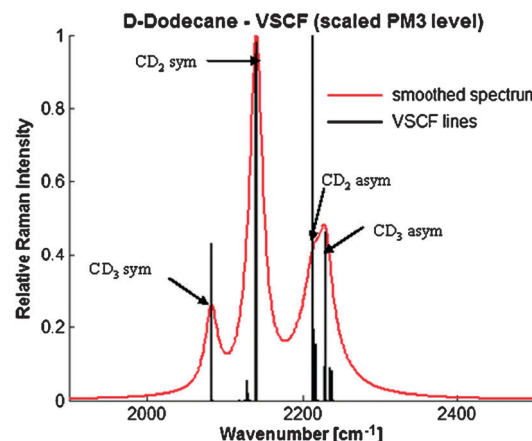


Fig. 7 The smoothed VSCF spectrum of a deuterated dodecane isotopomer calculated with the improved PM3 method (red curve) with the VSCF lines corresponding to all fundamental transition in this spectral range (black lines). The position of each black line corresponds to the transition frequency and the height denotes the transition relative Raman intensity (compared to the most intense transition).

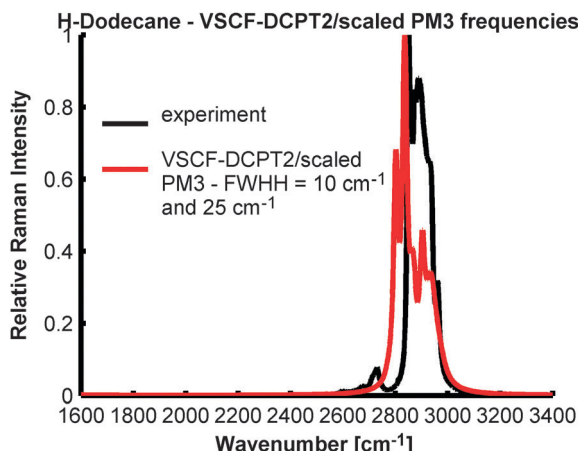


Fig. 8 The VSCF-DCPT2 spectra of a non-deuterated dodecane isotopomer calculated with the improved PM3 method (red curve) compared to experiment (black curve).

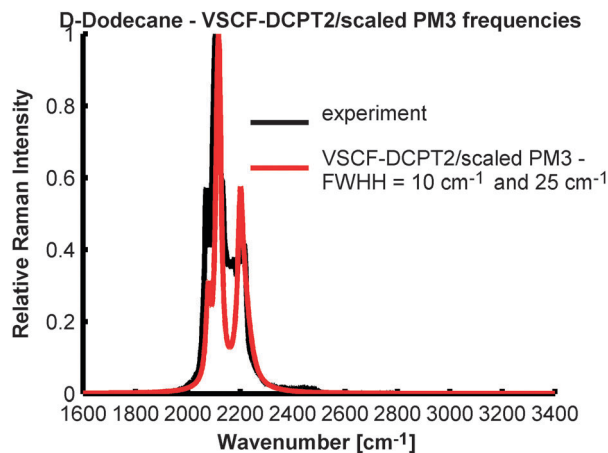


Fig. 9 The VSCF-DCPT2 spectra of a deuterated dodecane isotopomer calculated with the improved PM3 method (red curve) compared to experiment (black curve).

change their order (see Tables 2 and 4 and Fig. 5 and 7). For H-dodecane, the lowest vibrational frequencies correspond to symmetric CH_3 stretches (2772–2802 for VSCF-DCPT2 and 2850–2861 for VSCF), followed by symmetric CH_2 stretches (2824–2871 for VSCF-DCPT2 and 2862–2886 for VSCF) and asymmetric CH_3 stretches (2872–2904 for VSCF-DCPT2 and 2905–2941 for VSCF), the highest frequencies correspond to CH_2 asymmetric stretches (2935–2980 for VSCF-DCPT2 and 2940–2984 for VSCF), the frequencies expressed in cm^{-1} . Note that for VSCF-DCPT2 the separation of the vibrational frequencies is clearer than for simple VSCF. This effect is even more obvious for D-dodecane, where all mode types are clearly separated for VSCF-DCPT2, while for simple VSCF the asymmetric CD_3 and CD_2 stretches frequency ranges are mixed (2215–2230 for the former and 2214–2240 for the latter). The order of mode type frequency ranges is the same for H-dodecane and D-dodecane. The assignment of modes at the VSCF level (CH_3 symmetric, CH_2 symmetric, CH_3 asymmetric, and CH_2 asymmetric, counting from lower to higher frequencies), found for both isotopomers, differs from the conventional assignment, dating back to 1975.⁶⁸ The conventional empirically based assignments are as follows: the frequencies around 2850 cm^{-1} are attributed to CH_2 symmetric, the frequencies around 2890 cm^{-1} to CH_2 asymmetric, the frequencies around 2935 cm^{-1} to CH_3 symmetric, and the frequencies around 2960 cm^{-1} to CH_3 asymmetric modes. Note for example that the lowest level of VSCF assigns symmetric CH_3 vibrations to the region that corresponds to CH_2 symmetric bands according to the conventional assignment. Similarly, VSCF assigns CH_2 asymmetric modes to the frequency region that corresponds to CH_3 asymmetric transitions according to the conventional assignment, while the frequencies conventionally attributed to CH_2 asymmetric modes are close to the VSCF frequencies of CH_2 symmetric modes. On the other hand, the VSCF-DCPT2 predicts the CH_2 symmetric band at the expected place and the CH_3 symmetric band at the red edge of the spectrum (close to the position of the small red-edge peak found in experiment). Our results can thus bring a new light into the vibrational spectroscopy of the hydrocarbon stretches, however, the results show to be highly dependent on the quality of used potentials, *i.e.* the applied electronic structure method, and on the level of the anharmonic vibrational method. Therefore some additional calculations of CH stretches on a wider scale of molecules containing either CH_2 or CH_3 group, or both of them in various ratios, are advisable, preferably with high-level computational methods.

In the overall spectrum of H-dodecane we can see basically three clearly resolved peaks. Each of them is caused especially by one transition with a very high intensity which corresponds to one of the four mode types. The Raman intensities of all CH_3 asymmetric stretches are very small compared to the other modes and the spectral bands of these modes overlap with more intensive CH_2 asymmetric modes. The situation is similar for D-dodecane, however, in this case the highest Raman signal is caused by two transitions of roughly the same intensity and frequency, which explains why this peak is so dominant in the D-dodecane spectrum. Another difference is that for D-dodecane the CD_3 asymmetric stretches are somewhat stronger compared to other modes than was the

case of H-dodecane, and they are in principle visible in the spectrum. However, they can be still hardly resolved from CD_2 asymmetric stretches.

On the whole, keeping in mind the complexity of the actual system and conditions, the agreement between calculations and experiment is good both in Fig. 4 (VSCF) and in Fig. 8 (VSCF-DCPT2), although the nature of the agreement is somewhat different in the two cases. The fact that one gets a roughly simple level of agreement with two different approximate methods means that such calculations are robust for the intensity pattern. Note that while the two methods employed seem to give basically a similar level of accord with experiment, the underlying assignment is not the same for some of the frequencies. In the case of such a dense, strongly coupled band, the assignment in terms of localized transitions can depend sensitively on the vibrational method used. We emphasize, however, that agreement with the observed intensities is robust.

The nonreproduced red-edge experimental peak. In order to examine the origin of the Raman signal for a transition with a frequency of 2730 cm^{-1} , we have calculated the H-dodecane overtone frequencies of transitions likely to contribute to the spectrum in the region of our interest, which are especially CH_2 and CH_3 scissoring vibrations. These vibrations are very likely to interact with the C–H stretches, which can lead to a relatively high intensity of such transitions due to resonance. Six modes of that kind were found, their frequencies are shown in Table 3. Indeed, these frequencies correspond to the discussed red-edge experimental peak. This assumption can be verified by applying Raman intensity calculations which require computations beyond the harmonic approximation, which has not been possible with our software so far. A similar calculation was made for D-dodecane. In this case just three modes of this kind were found—see Table 5. The smaller number of transitions likely to cause the Raman signal is a possible reason why the red-edge peak is not present in D-dodecane experimental spectra.

An alternative explanation for this peak is that it is caused only by fundamental transitions with the smallest frequencies. This assumption is supported by the VSCF-DCPT2 spectral shape, containing several transitions with frequencies approaching the position of the experimental peak of interest, and also by the absence of the peak in the D-dodecane spectrum. In this case, this peak would be caused by degeneracy effects. However, the agreement with experiment for this part of the spectrum is considerably worse than for the other parts and it is thus not possible to be sure that the assignment

Table 3 Vibrational modes possibly contributing to the vibrational spectra of non-deuterated dodecane in the region of C–H stretch fundamental transitions

Overtones		Fundamental frequency/ cm^{-1}	Overtone frequency/ cm^{-1}
Mode	Type		
78	CH_2 and CH_3 scissors	1363	2721
79	CH_3 scissors	1364	2720
80	CH_2 scissors	1367	2731
81	CH_2 and CH_3 scissors	1366	2728
82	CH_2 scissors	1373	2743
83	CH_2 scissors	1373	2745

Table 4 The vibrational frequencies of the CD₂ and CD₃ stretching modes in the deuterated dodecane molecule at both the harmonic and anharmonic levels. The mode numbers correspond to the harmonical modes listed in Table 2 which were assigned to them

Mode	Type	MP2 harmonic	Imp. PM3-VSCF	Imp. PM3- VSCF_DCPT2	Raman intensities
89	CD ₂ sym	2223	2127	2122	0
90	CD ₂ sym	2224	2129	2109	10
91	CD ₂ sym	2227	2128	2124	0
92	CD ₂ sym	2223	2128	2095	1
93	CD ₂ sym	2230	2140	2114	186
94	CD ₂ sym	2224	2120	2112	0
95	CD ₂ sym	2225	2129	2112	3
96	CD ₂ sym	2226	2133	2128	0
97	CD ₂ sym	2237	2142	2120	195
98	CD ₂ sym	2237	2130	2121	3
99	CD ₃ sym	2212	2083	2078	0
100	CD ₃ sym	2212	2084	2077	85
101	CD ₂ asym	2293	2214	2211	198
102	CD ₂ asym	2294	2214	2211	0
103	CD ₂ asym	2296	2217	2214	31
104	CD ₂ asym	2300	2220	2217	0
105	CD ₂ asym	2305	2228	2226	18
106	CD ₂ asym	2310	2231	2230	0
107	CD ₂ asym	2315	2235	2232	18
108	CD ₂ asym	2319	2238	2234	0
109	CD ₂ asym	2321	2239	2234	16
110	CD ₂ asym	2323	2240	2236	0
111	CD ₃ asym	2349	2215	2198	38
112	CD ₃ asym	2349	2215	2199	0
113	CD ₃ asym	2352	2229	2200	16
114	CD ₃ asym	2352	2230	2201	85

Table 5 Vibrational modes possibly contributing to the vibrational spectra of deuterated dodecane in the region of C–D stretch fundamental transitions

Mode	Type	Fundamental frequency/cm ⁻¹	Overtone frequency/cm ⁻¹
75	CD ₂ and CD ₃ scissors	1026	2051
76	CD ₂ and CD ₃ scissors	1030	2060
77	CD ₂ and CD ₃ scissors	1033	2065

of the symmetric CH₃ stretches to this peak is correct. Moreover, the predicted intensity of these transitions is much stronger than is observed in the experimental peak. In the absence of clear evidence, it can be said that at the resolution of the experiments there seems to be no important degeneracy effects in the spectrum. In summary, at the present state of the research, a definite explanation for the red-edge peak in H-dodecane (and the absence thereof for D-dodecane) cannot be given. A decision between two possible interpretations proposed above can best be reached by future higher-resolution experiments.

4. Concluding remarks

The main message of this article is that first-principles anharmonic vibrational calculations of the Raman spectra of long-chain hydrocarbons are feasible, and yield on the whole good agreement with experiments, carried out for the liquid phase and at ambient temperatures. The results seem to us to suggest that such calculations should be equally successful for any systems of this class, rendering many applications possible. It seems that providing a unique assignment from such calculations

is less reliable than the accord with experiment on the observed spectrum. The reason is that in a dense, quasi-degenerate, strongly-coupled band, interpretation in terms of localized modes is sensitive to details, such as electronic potentials and the level of anharmonicity treatment. However, the approach taken here seems to provide a powerful tool for the quantitative interpretation of the hydrogenic stretching band in hydrocarbons, and perhaps also in more complex systems where other types of biomolecules (proteins, saccharides) are present jointly with compounds containing alkyl chains. Raman analysis of hydrocarbon mixtures is a potential application, as is in principle the study of proteins or saccharides in lipid membranes. Future work is planned in these directions.

A theoretical implication of the results is that anharmonic effects in the CH stretching band of hydrocarbons play, not surprisingly, a major role, which is well described by VSCF. On the other hand, degeneracy effects do not seem very important, given that VSCF variants that do not include Fermi resonances and other corrections for degeneracy gave very good agreement with experiment. The only exception is the red-edge peak of H-dodecane, which could be either due to a degeneracy effect (as described by VSCF-DCPT2), or it could be due to a bending overtone. In either case, future high resolution experiments, *e.g.* in molecular beams or in cryogenic matrices, may probably throw light on the situation, and yield evidence on other possible manifestations of resonance effects in the CH band of hydrocarbons.

Acknowledgements

Research at the Hebrew University was supported by resources of the Saerree K. and Louis P. Fiedler Chair in chemistry (RBG). JŠ thanks the HU for a postdoctoral Golda Meir Fellowship for the years 2009–2010 and 2010–2011. Thanks also to Dr Brina Brauer for providing us with source codes.

References

- 1 J. X. Cheng and X. S. Xie, Coherent anti-Stokes Raman Scattering Microscopy: Instrumentation, Theory and Applications, *J. Phys. Chem. B*, 2004, **108**(3), 827–840.
- 2 C. L. Evans and X. S. Xie, Coherent Anti-Stokes Raman Scattering Microscopy: Chemical Imaging for Biology and Medicine, *Annu. Rev. Anal. Chem.*, 2008, **1**, 883–909.
- 3 C. W. Freudiger, W. Min, B. G. Saar, S. Lu, G. R. Holton, C. He, J. C. Tsai, J. X. Kang and X. S. Xie, Label-Free Biomedical Imaging with High Sensitivity by Stimulated Raman Scattering Microscopy, *Science*, 2008, **322**, 1857–1861.
- 4 J. X. Cheng, A. Volkmer, L. D. Book and X. S. Xie, Multiplex coherent anti-Stokes Raman scattering microspectroscopy and study of lipid vesicles, *J. Phys. Chem. B*, 2002, **106**(34), 8493–8498.
- 5 R. Lu, W. Gan, B. H. Wu, Z. Zhang, Y. Guo and H. F. Wang, C–H stretching vibrations of methyl, methylene and methine groups at the vapor/alcohol ($n = 1$ –8) interfaces, *J. Phys. Chem. B*, 2005, **109**(29), 14118–14129.
- 6 T. Hellerer, T. Axäng, C. Brackmann, P. Hillertz, M. Pilon and A. Enejder, Monitoring of lipid storage in *Caenorhabditis elegans* using coherent anti-Stokes Raman scattering (CARS) microscopy, *Proc. Natl. Acad. Sci. U. S. A.*, 2007, **104**(37), 14658–14663.
- 7 T. B. Huff and J. X. Cheng, *In vivo* coherent anti-Stokes Raman scattering imaging of sciatic nerve tissues, *J. Microsc.*, 2007, **225**(2), 175–182.
- 8 X. Nan, J. X. Cheng and X. S. Xie, Vibrational imaging of lipid droplets in live fibroblast cells with coherent anti-Stokes Raman scattering microscopy, *J. Lipid Res.*, 2003, **44**(11), 2202–2208.

- 9 H. W. Wang, I. M. Langohr, M. Sturek and J. X. Cheng, Imaging and quantitative analysis of atherosclerotic lesions by CARS-based multimodal nonlinear optical microscopy, *Arterioscler., Thromb., Vasc. Biol.*, 2009, **29**(9), 1342–1348.
- 10 B. P. Gaber and W. L. Peticolas, On the quantitative interpretation of biomembrane structure by Raman spectroscopy, *Biochim. Biophys. Acta, Biomembr.*, 1977, **465**(2), 260–274.
- 11 R. G. Snyder, Vibrational study of the chain conformation of the liquid *n*-paraffins and molten polyethylene, *J. Chem. Phys.*, 1967, **47**(4), 1316–1360.
- 12 R. G. Snyder, S. L. Hsu and S. Krimm, Vibrational spectra in the C–H stretching region and the structure of the polymethylene chain, *Spectrochim. Acta*, 1978, **34A**(12), 395–406.
- 13 R. G. Snyder, H. L. Strauss and C. A. Elliger, C–H stretching modes and structure of *n*-alkyl chains 1. Long, disordered chains, *J. Phys. Chem.*, 1982, **86**(26), 5145–5150.
- 14 V. R. Kodati, R. El-Jastimi and M. Lafleur, Contribution of the intermolecular coupling and librotorsional mobility in the methylene stretching modes on the infrared spectra of acyl chains, *J. Phys. Chem.*, 1994, **98**(47), 12191–12197.
- 15 H. A. Rinia, K. N. J. Burger, M. Bonn and M. Müller, Quantitative Label-Free Imaging of Lipid Composition and Packing of Individual Cellular Lipid Droplets Using Multiplex CARS Microscopy, *Biophys. J.*, 2008, **95**(10), 4908–4914.
- 16 G. W. H. Wurpel, H. A. Rinia and M. Müller, Imaging orientational order and lipid density in multilamellar vesicles with multiplex CARS microscopy, *J. Microsc.*, 2005, **218**(1), 37–45.
- 17 M. T. Devlin and I. W. Levin, Raman spectroscopic studies of the packing properties of mixed dihexadecyl- and dipalmitoyl-phosphotidylcholine bilayer dispersions, *Biochemistry*, 1989, **28**(22), 8912–8920.
- 18 S. P. Verma and D. F. H. Wallach, *Raman spectroscopy of lipids and membranes*, in *Biomembrane structure and function*, ed. D. Chapman, Verlag Chemie, Basel, 1984, pp. 167–198.
- 19 E. B. Wilson, J. C. Decius and P. C. Cross, *Molecular Vibrations*, McGraw-Hill, New York, 1955.
- 20 T. Miyazawa, T. Shimanouchi and S.-I. Mizushima, Normal vibrations of *N*-methyl acetamide, *J. Chem. Phys.*, 1958, **29**, 611–616.
- 21 W. D. Gwinn, Normal Coordinates—General Theory, Redundant Coordinates and General Analysis Using Electronic Computers, *J. Chem. Phys.*, 1971, **55**(2), 477–481.
- 22 N. G. Mirkin and S. Krimm, *Ab initio* vibrational analysis of hydrogen-bonded *trans*- and *cis*-*N*-methylacetamide, *J. Am. Chem. Soc.*, 1991, **113**, 9742–9747.
- 23 A. G. Csaszar, On the structures of free glycine and alpha-alanine, *J. Mol. Struct.*, 1995, **346**, 141–152.
- 24 A. G. Csaszar, Conformers of gaseous alpha-alanine, *J. Phys. Chem.*, 1996, **100**(9), 3541–3551.
- 25 A. Roitberg, R. B. Gerber, R. Elber and M. A. Ratner, Anharmonic Wavefunctions of Proteins—Quantum Self-Consistent-Field Calculations of Bpti, *Science*, 1995, **268**(5215), 1319–1322.
- 26 B. Brauer, R. B. Gerber, M. Kabeláč, P. Hobza, J. M. Bakker, A. G. A. Riziq and M. S. de Vries, Vibrational spectroscopy of the G·C base pair: Experiment, harmonic and anharmonic calculations and the nature of the anharmonic couplings, *J. Phys. Chem. A*, 2005, **109**(31), 6974–6984.
- 27 B. Brauer, F. Dubnikova, Y. Zeiri, R. Kosloff and R. B. Gerber, Vibrational spectroscopy of triacetone triperoxide (TATP): Anharmonic fundamentals, overtones and combination bands, *Spectrochim. Acta, Part A*, 2008, **71**(4), 1438–1445.
- 28 C. Cappelli, S. Monti, G. Scalmani and V. Barone, On the Calculation of Vibrational Frequencies for Molecules in Solution Beyond the Harmonic Approximation, *J. Chem. Theory Comput.*, 2010, **6**(5), 1660–1669.
- 29 L. Jiang, T. Wende, R. Bergmann, G. Meijer and K. R. Asmis, Gas-phase Vibrational Spectroscopy of Microhydrated Magnesium Nitrate Ions [MgNO₃(H₂O)(1–4)], *J. Am. Chem. Soc.*, 2010, **132**(21), 7398–7404.
- 30 J. O. Jung and R. B. Gerber, Vibrational wave functions and spectroscopy of (H₂O)(*n*), *n* = 2, 3, 4, 5: Vibrational self-consistent field with correlation corrections, *J. Chem. Phys.*, 1996, **105**(23), 10332–10348.
- 31 J. P. P. Stewart, Optimization of parameters for semiempirical methods. I. Method, *J. Comput. Chem.*, 1989, **10**(2), 209–220.
- 32 B. Brauer, G. M. Chaban and R. B. Gerber, Spectroscopically-tested, improved, semi-empirical potentials for biological molecules: Calculations for glycine, alanine and proline, *Phys. Chem. Chem. Phys.*, 2004, **6**(10), 2543–2556.
- 33 N. L. Allinger, Y. H. Yuh and J.-H. Lii, Molecular Mechanics. The MM3 Force Field for Hydrocarbons. 1, *J. Am. Chem. Soc.*, 1989, **111**(23), 8551–8566.
- 34 Ponder and J. W. Tinker, *Software Tools for Molecular Design*, 3.8, Washington University School of Medicine, Saint Louis, 2000.
- 35 M. W. Schmidt, K. K. Baldridge, J. A. Boatz, S. T. Elbert, M. S. Gordon, J. H. Jensen, S. Koseki, N. Matsunaga, K. A. Nguyen, S. J. Su, T. L. Windus, M. Dupuis and J. A. Montgomery, General Atomic and Molecular Electronic-Structure System, *J. Comput. Chem.*, 1993, **14**(11), 1347–1363.
- 36 C. Møller and M. S. Plesset, Note on an approximation treatment for many-electron systems, *Phys. Rev.*, 1934, **46**(7), 618–622.
- 37 T. H. Dunning, Jr., Gaussian Basis Sets for Use in Correlated Molecular Calculations. I. The Atoms Boron through Neon and Hydrogen, *J. Chem. Phys.*, 1989, **90**(2), 1007–1023.
- 38 R. A. Kendall, T. H. Dunning, Jr. and R. J. Harrison, Electron affinities of the first-row atoms revisited. Systematic basis sets and wave functions, *J. Chem. Phys.*, 1992, **96**(9), 6796–6806.
- 39 J. M. Bowman, Self-Consistent-Field Energies and Wavefunctions for Coupled Oscillators, *J. Chem. Phys.*, 1978, **68**(2), 608–610.
- 40 J. M. Bowman, The Self-Consistent-Field Approach to Polyatomic Vibrations, *Acc. Chem. Res.*, 1986, **19**(7), 202–208.
- 41 R. B. Gerber and M. A. Ratner, Semi-Classical Self-Consistent-Field (Sc Scf) Approximation for Eigenvalues of Coupled-Vibration Systems, *Chem. Phys. Lett.*, 1979, **68**(1), 195–198.
- 42 R. B. Gerber and M. A. Ratner, Self-Consistent-Field Methods for Vibrational Excitations in Polyatomic Systems, *Adv. Chem. Phys.*, 1988, **70**, 97–132.
- 43 S. K. Gregurick, E. Fredj, R. Elber and R. B. Gerber, Vibrational spectroscopy of peptides and peptide–water complexes: Anharmonic coupled-mode calculations, *J. Phys. Chem. B*, 1997, **101**(42), 8595–8606.
- 44 S. K. Gregurick, J. H.-Y. Liu, D. A. Brant and R. B. Gerber, Anharmonic vibrational self-consistent field calculations as an approach to improving force fields for monosaccharides, *J. Phys. Chem. B*, 1999, **103**(7), 3476–3488.
- 45 G. M. Chaban, J. O. Jung and R. B. Gerber, Anharmonic vibrational spectroscopy of glycine: Testing of *ab initio* and empirical potentials, *J. Phys. Chem. A*, 2000, **104**(44), 10035–10044.
- 46 Z. Bihary, R. B. Gerber and V. A. Apkarian, Vibrational self-consistent field approach to anharmonic spectroscopy of molecules in solids: Application to iodine in argon matrix, *J. Chem. Phys.*, 2001, **115**(6), 2695–2701.
- 47 R. B. Gerber, B. Brauer, S. K. Gregurick and G. M. Chaban, Calculation of anharmonic vibrational spectroscopy of small biological molecules, *PhysChemComm*, 2002, **5**, 142–150.
- 48 J. Neugebauer and B. A. Hess, Fundamental vibrational frequencies of small polyatomic molecules from density-functional calculations and vibrational perturbation theory, *J. Chem. Phys.*, 2003, **118**(16), 7215–7225.
- 49 C. Espinoza, J. Szczepanski, M. Vala and N. C. Polfer, Glycine and Its Hydrated Complexes: A Matrix Isolation Infrared Study, *J. Phys. Chem. A*, 2010, **114**(18), 5919–5927.
- 50 P. Seidler, T. Kaga, K. Yagi, O. Christiansen and K. Hirao, On the coupling strength in potential energy surfaces for vibrational calculations, *Chem. Phys. Lett.*, 2009, **483**(1–3), 138–142.
- 51 G. M. Chaban, J. O. Jung and R. B. Gerber, Anharmonic vibrational spectroscopy of hydrogen-bonded systems directly computed from *ab initio* potential surfaces: (H₂O)(*n*), *n* = 2, 3; Cl-(H₂O)(*n*), *n* = 1, 2; H + (H₂O)(*n*), *n* = 1, 2; H₂O-CH₃OH, *J. Phys. Chem. A*, 2000, **104**(12), 2772–2779.
- 52 M. B. Shundalov, G. A. Pitsevich, M. A. Ksenofontov and D. S. Umreiko, Quantum-chemical calculations of the structure, vibrational spectra and torsional and inversion potentials of methylcarbamate, *J. Appl. Spectrosc.*, 2009, **76**(3), 325–333.
- 53 O. Christiansen and J. M. Luis, Beyond vibrational self-consistent-field methods: Benchmark calculations for the fundamental vibrations of ethylene, *Int. J. Quantum Chem.*, 2005, **104**, 667–680.
- 54 A. T. Kowal, Computational study of the equilibrium geometry and anharmonic vibrational spectra of PbX₂·NO and

- PbX₂···ON (X = F, Cl, Br, I) complexes, *Mol. Phys.*, 2010, **108**(12), 1665–1675.
- 55 R. B. Gerber, G. M. Chaban, B. Brauer and Y. Miller, *Theory and applications of computational chemistry: the first 40 years*, 2005, ch. 9, pp. 165–193.
- 56 I. Suwan and R. B. Gerber, VSCF in internal coordinates and the calculations of anharmonic torsional mode transitions, *Chem. Phys.*, 2010, **373**, 267–273.
- 57 J. O. Jung and R. B. Gerber, Vibrational wave functions and energy levels of large anharmonic clusters: A vibrational SCF study of Ar₁₃, *J. Chem. Phys.*, 1996, **105**(24), 10682–10690.
- 58 L. S. Norris, M. A. Ratner, A. E. Roitberg and R. B. Gerber, Moller–Plesset perturbation theory applied to vibrational problems, *J. Chem. Phys.*, 1996, **105**(24), 11261–11267.
- 59 L. Pele, B. Brauer and R. B. Gerber, Acceleration of correlation-corrected vibrational self-consistent field calculation times for large polyatomic molecules, *Theor. Chem. Acc.*, 2007, **117**(1), 69–72.
- 60 L. Pele and R. B. Gerber, On the number of significant mode-mode anharmonic couplings in vibrational calculations: Correlation-corrected vibrational self-consistent field treatment of di-, tri- and tetrapeptides, *J. Chem. Phys.*, 2008, **128**(16), 165105.
- 61 D. M. Benoit, Efficient correlation-corrected vibrational self-consistent field computation of OH-stretch frequencies using a low-scaling algorithm, *J. Chem. Phys.*, 2006, **125**(24), 244110–244111.
- 62 N. Matsunaga, G. M. Chaban and R. B. Gerber, Degenerate perturbation theory corrections for the vibrational self-consistent field approximation: Method and applications, *J. Chem. Phys.*, 2002, **117**(8), 3541–3547.
- 63 P. Daněček and P. Bouř, Comparison of the Numerical Stability of Methods for Anharmonic Calculations of Vibrational Molecular Energies, *J. Comput. Chem.*, 2007, **28**(10), 1617–1624.
- 64 I. Respondék and D. M. Benoit, Fast degenerate correlation-corrected vibrational self-consistent field calculations of the vibrational spectrum of 4-mercaptopuridine, *J. Chem. Phys.*, 2009, **131**(5), 054109.
- 65 G. M. Chaban, J. O. Jung and R. B. Gerber, *Ab initio* calculation of anharmonic vibrational states of polyatomic systems: Electronic structure combined with vibrational self-consistent field, *J. Chem. Phys.*, 1999, **111**(5), 1823–1829.
- 66 A. A. Adesokan, E. Fredj, E. C. Brown and R. B. Gerber, Anharmonic vibrational frequency calculations of 5,6-dihydro-uracil and its complex with water: testing improved semiempirical potentials for biological molecules, *Mol. Phys.*, 2005, **103**(11–12), 1505–1520.
- 67 A. A. Adesokan, D. Pan, E. Fredj, R. A. Mathies and R. B. Gerber, Anharmonic vibrational calculations modeling the Raman spectra of intermediates in the photoactive yellow protein (PYP) photocycle, *J. Am. Chem. Soc.*, 2007, **129**(15), 4584–4594.
- 68 R. C. Spiker and I. W. Levin, Raman-Spectra and Vibrational Assignments for Dipalmitoyl Phosphatidylcholine and Structurally Related Molecules, *Biochim. Biophys. Acta, Lipids Lipid Metab.*, 1975, **388**(3), 361–373.